Annals of the Academy of Romanian Scientists
Series on Engineering Sciences
ISSN 2066-8570 Volume **15**, Number **1**/**2023**

CLUSTER ANALYSIS APPROACH FOR IDENTIFYING OPTIMAL CUTTING PARAMETERS IN END MILLING OF ALUMINUM ALLOY 7136 FOR IMPROVED SURFACE ROUGHNESS

Aurel Mihail ȚÎȚU[1,2], Constantin OPREAN[3,4], Alina Bianca POP[5]

Rezumat. *Analiza clusterelor este utilizată ca principala inovație metodologică în acest studiu pentru a determina cei mai buni parametri de așchiere pentru rugozitatea suprafeței la frezarea aliajului de aluminiu 7136. Conform concluziilor, fiecare cluster reprezintă un set unic de circumstanțe de prelucrare, cum ar fi o viteză de așchiere și o adâncime de așchiere mică cu un avans pe dinte mare și o rugozitate a suprafeței mare sau o viteză și o adâncime de așchiere mare cu un avans pe dinte mic și o rugozitate a suprafeței mică. Rezultatele sunt evaluate în raport cu literatura de specialitate și sunt oferite sugestii pentru direcțiie de cercetare viitoare. Această cercetare poate contribui la îmbunătățirea aspectului și a utilizării practice a componentelor prelucrate.*

Abstract. *Three cutting parameters are investigated in this study for their effect on the surface quality of aluminum alloy 7136 end milled. The major goal of the study is to use cluster analysis to discover the ideal cutting parameter combination to get the lowest surface roughness achievable. This paper examines cutting parameters and surface roughness for aluminum alloy end milling operations, finds literature gaps, and provides the experimental setup and research methodology. According to the findings, the data points are split into three categories depending on the characteristics of each individual data point. The findings are evaluated considering contemporary literature, and recommendations for further research are provided. As a consequence of this research, it is now clear how to optimize the cutting settings for end milling aluminum alloy 7136, potentially improving the usability and aesthetics of machined components.*

Keywords: Cluster analysis, cutting parameters, end-milling process, Al7136, surface roughness.

DOI https://doi.org/10.56082/annalsarscieng.2023.1.124

[1]Professor dr. eng. and dr. ec. -mg., Dr. Habil. Dr. h. c., Lucian Blaga University of Sibiu, 10, Victoriei Street, Sibiu, România (mihail.titu@ulbsibiu.ro).
[2]The Academy of Romanian Scientists, 54, Splaiul Independenței, Sector 5, Bucharest, Romania.
[3]Prof. univ. emerit dr. eng. Dr. h. c., Lucian Blaga University of Sibiu, 10, Victoriei Street, Sibiu, România, (constantin.oprean@ulbsibiu.ro).
[4]The Academy of Romanian Scientists, 54, Splaiul Independenței, Sector 5, Bucharest, Romania.
[5]As/Professor, Technical University of Cluj-Napoca, North University Center of Baia Mare, 62A, Victor Babeş Street, Baia Mare, Romania, (bianca.bontiu@gmail.com).

1. Introduction

Determining the surface roughness of machined components in order to assess their quality and usefulness is a critical procedure in the manufacturing business. The link between surface roughness and various machining processes' cutting parameters has been investigated. More research is needed to minimize surface roughness and optimize cutting settings for end milling aluminum alloys.

[1] explored how cutting parameters influenced surface integrity while milling aircraft aluminum alloys. They observed that the most important characteristics were cutting speed and feed rate, with depth of cut having the least influence on surface roughness.

[2] provides a method for evaluating surface roughness in aluminum alloy end milling using adaptive neuro-fuzzy inference. They observed that the feed rate, depth of cut, and cutting speed all influenced surface roughness.

[3] investigated how the surface roughness of hardened tool steel altered during high-speed machining. They observed that the feed rate, depth of cut, and cutting speed all had an effect on surface roughness.

When high-speed milling an aluminum alloy, [4] employed the response surface technique to improve surface roughness. They observed that the feed rate, depth of cut, and cutting speed all had an effect on surface roughness.

[5] modified the machining parameters and improved surface roughness by end milling aluminum alloy 6063-T6.

The feed rate, spindle speed, and depth of cut all had a substantial influence on the surface roughness, they observed.

Finally, [6] investigated the efficacy of coated carbide tools for cutting titanium alloy. They observed that tool coating influenced tool wear and surface roughness significantly. It has been demonstrated that tools coated with TiAlN have superior surface finishes and less tool wear than other materials.

[7] examined how surface roughness, cutting pressures, and tool wear were impacted by cutting parameters while milling Al6061 alloy. While a faster feed rate and faster cutting speed increased surface roughness and cutting pressures, a shallower cut decreased tool wear.

Using the Taguchi approach, [8] improves cutting parameters when milling aluminum alloy 6063, similar to [5].

They observed that feed rate, spindle speed, and cut depth all had a substantial impact on surface roughness.

Using the Taguchi approach, [9] investigated how milling settings influenced cutting forces and surface roughness. They concluded that feed rate, spindle speed, and cut depth all had a substantial impact on surface roughness.

Another approach for simulating surface roughness in milling is response surface technology (RSM). [10] utilized Taguchi-based RSM to model surface roughness during aluminum alloy milling. They discovered that cutting speed and feed rate had the greatest effect on surface roughness.

[11] employed RSM to estimate surface roughness during end milling aluminum alloy. They discovered that feed rate and cutting speed had the largest impact on surface roughness, whereas depth of cut had little to no impact.

[12] assessed surface abrasion during end milling an aluminum alloy using an adaptive neuro-fuzzy inference system (ANFIS). They discovered that feed rate and cutting speed had the largest impact on surface roughness, whereas depth of cut had little to no impact.

This study explored the influence of tool coatings on surface integrity during milling in addition to simulating surface roughness. [12,13] investigated surface integrity by grinding aluminum with a range of coated carbide tools.

More research is needed to improve the efficiency of selecting these parameters and the precision of surface roughness prediction models in aluminum milling. The findings of this literature review, taken as a whole, give significant insights into the current state of research in this field and offer practitioners useful guidance for improving their milling methods for aluminum alloys.

Our research aims to improve the cutting parameters of end milling operations for aluminum alloy 7136 by addressing information gaps.

The lack of studies on the optimization of cutting parameters for surface roughness in end milling of aluminum alloys, as well as the use of cluster analysis to identify optimal cutting parameters, encouraged us to conduct this research.

The study's most notable methodological achievement is the use of cluster analysis to determine the ideal cutting parameters for surface roughness during end milling of aluminum alloy 7136. The primary goals of this study are to evaluate the effects of various cutting parameters, such as cutting speed, depth of cut, and feed per tooth, on surface roughness when end milling aluminum alloy 7136, and to determine the best set of cutting parameters for achieving the lowest surface roughness.

The following is how the paper is formatted: In the first chapter, we discuss the research on cutting parameters and surface roughness in aluminum alloy end milling operations. The research strategy and experimental design are discussed in the second part. In the third part, we present our testing findings as well as a data cluster analysis. In the concluding section, we examine the significance of our findings, the study's limitations, and future research recommendations.

2. Materials and methods

2.1. Material Used

Al7136 is the substance that was utilized in the tests. A heat-treatable alloy from the 7xxx family of aluminum alloys is called Al7136-T76511. An outstanding stress corrosion cracking resistance and superior machinability characterize this high-strength alloy. The following are some properties of Al7136-T76511:

Chemical Make-Up: The alloy has a high aluminum content and trace amounts of other metals such as zinc, magnesium, and copper. The exact composition of the alloy may vary depending on the manufacturer, but typically it has 5-6% zinc, 2-3% magnesium, and 1% copper.

Mechanical Features: The alloy has a high strength-to-weight ratio and can withstand significant stresses. The mechanical properties can be improved by heat treatment. The alloy's yield strength is normally in the range of 490 to 510 MPa (70-74 ksi), while the tensile strength typically varies from 590 to 620 MPa (85 to 90 ksi) for the T76511 temper condition.

The alloy has a melting point of 640 °C (1184 °F), and its density is approximately 2.8 g/cm3.

Due to its great machinability, the alloy is suitable for use in a range of applications that need high strength and excellent surface quality.

High-strength aluminum alloy Al7136-T76511 has excellent stress corrosion cracking resistance and generally acceptable machinability. High-performance sporting items, car parts, and aircraft components are typically used in its manufacture [14].

2.2. Experimental Setup

The HAAS-VF2 CNC machine is employed. In industrial applications, the Haas VF-2 vertical machining center is often used to produce machined components from a variety of materials. The apparatus was created by the renowned CNC machine maker Haas Automation, which is noted for its durability and precision [15].

The Haas VF-2 features a 40-taper spindle with a maximum speed of 12,000 RPM. A 30-horsepower vector drive motor that can deliver a lot of torque at low speeds for efficient cutting powers the spindle. The machine's high traverse rate of 1,400 IPM and maximum feed rate of 1,000 IPM enable quick positioning and machining.

The milling tool SECO R217.69-1616.0-09-2AN has been specified for this application. This tool is one inch in diameter and contains nine cutting teeth. The tool is designed to be used in high-speed machining operations and is made of carbide for improved performance and durability [16].

The precise cutting parameters for this tool on the Haas VF-2 would depend on the application and material being machined. While cutting aluminum alloy 7136, this tool is typically configured to spin at 10,000 RPM, feed at 100 IPM, and cut at 0.1-inch depths. These parameters would need to be modified based on the material properties, the form of the workpiece, and the desired surface finish.

2.3. Experimental Design

The experiment's goal is to assess the effects of cutting speed, depth of cut, and feed per tooth on the Al7136 material's surface roughness during an end milling operation. The experiment is set up using a complete factorial design with 150 experiments, each with three duplicates, and a total of 450 data points (table 1).

Independent Variables:

- Cutting speed [m/min]
- Depth of cut [mm]
- Feed per tooth [mm/tooth]

Dependent Variable:

- Surface roughness (Ra measurements) [µm]

Table 1. Surface roughness values for different cutting parameters

exp	*v [m/min]*	*ap [mm]*	*fz [mm/tooth]*	*Ra [µm]*		*exp*	*v [m/min]*	*ap [mm]*	*fz [mm/tooth]*	*Ra [µm]*
1	495	2	0.04	0.186		76	610	2	0.04	0.533
2	495	2	0.06	0.216		77	610	2	0.06	0.475
3	495	2	0.08	0.219		78	610	2	0.08	1.035
4	495	2	0.11	0.217		79	610	2	0.11	0.554
5	495	2	0.14	0.286		80	610	2	0.14	0.546
6	495	2.5	0.04	0.189		81	610	2.5	0.04	0.547
7	495	2.5	0.06	0.173		82	610	2.5	0.06	0.535
8	495	2.5	0.08	0.165		83	610	2.5	0.08	0.696
9	495	2.5	0.11	0.215		84	610	2.5	0.11	0.531

10	495	2.5	0.14	0.236	85	610	2.5	0.14	0.481
11	495	3	0.04	0.197	86	610	3	0.04	0.509
12	495	3	0.06	0.366	87	610	3	0.06	0.553
13	495	3	0.08	0.180	88	610	3	0.08	0.596
14	495	3	0.11	0.193	89	610	3	0.11	0.520
15	495	3	0.14	0.464	90	610	3	0.14	0.458
16	495	3.5	0.04	0.188	91	610	3.5	0.04	0.679
17	495	3.5	0.06	0.183	92	610	3.5	0.06	0.631
18	495	3.5	0.08	0.168	93	610	3.5	0.08	0.543
19	495	3.5	0.11	0.239	94	610	3.5	0.11	0.581
20	495	3.5	0.14	0.252	95	610	3.5	0.14	0.614
21	495	4	0.04	0.191	96	610	4	0.04	0.722
22	495	4	0.06	0.188	97	610	4	0.06	0.970
23	495	4	0.08	0.176	98	610	4	0.08	0.540
24	495	4	0.11	0.218	99	610	4	0.11	0.498
25	495	4	0.14	0.179	100	610	4	0.14	0.416
26	530	2	0.04	0.186	101	660	2	0.04	0.503
27	530	2	0.06	0.219	102	660	2	0.06	0.686
28	530	2	0.08	0.183	103	660	2	0.08	0.667
29	530	2	0.11	0.311	104	660	2	0.11	0.490
30	530	2	0.14	0.586	105	660	2	0.14	0.740
31	530	2.5	0.04	0.200	106	660	2.5	0.04	0.586
32	530	2.5	0.06	0.219	107	660	2.5	0.06	0.644
33	530	2.5	0.08	0.224	108	660	2.5	0.08	0.653
34	530	2.5	0.11	0.277	109	660	2.5	0.11	0.613
35	530	2.5	0.14	0.268	110	660	2.5	0.14	0.674
36	530	3	0.04	0.206	111	660	3	0.04	0.544
37	530	3	0.06	0.208	112	660	3	0.06	0.544
38	530	3	0.08	0.417	113	660	3	0.08	0.541
39	530	3	0.11	0.252	114	660	3	0.11	0.577
40	530	3	0.14	0.246	115	660	3	0.14	0.606
41	530	3.5	0.04	0.222	116	660	3.5	0.04	0.529
42	530	3.5	0.06	0.241	117	660	3.5	0.06	0.652
43	530	3.5	0.08	0.178	118	660	3.5	0.08	0.630
44	530	3.5	0.11	0.234	119	660	3.5	0.11	0.456
45	530	3.5	0.14	0.244	120	660	3.5	0.14	0.604
46	530	4	0.04	0.236	121	660	4	0.04	0.602
47	530	4	0.06	0.219	122	660	4	0.06	0.528

48	530	4	0.08	0.199	123	660	4	0.08	0.499
49	530	4	0.11	0.215	124	660	4	0.11	0.601
50	530	4	0.14	0.271	125	660	4	0.14	0.504
51	570	2	0.04	0.439	126	710	2	0.04	0.538
52	570	2	0.06	0.514	127	710	2	0.06	0.538
53	570	2	0.08	0.547	128	710	2	0.08	0.579
54	570	2	0.11	0.434	129	710	2	0.11	0.501
55	570	2	0.14	0.354	130	710	2	0.14	0.565
56	570	2.5	0.04	0.473	131	710	2.5	0.04	0.554
57	570	2.5	0.06	0.509	132	710	2.5	0.06	0.544
58	570	2.5	0.08	0.529	133	710	2.5	0.08	0.595
59	570	2.5	0.11	0.466	134	710	2.5	0.11	0.543
60	570	2.5	0.14	0.393	135	710	2.5	0.14	0.503
61	570	3	0.04	0.542	136	710	3	0.04	0.539
62	570	3	0.06	0.497	137	710	3	0.06	0.506
63	570	3	0.08	0.547	138	710	3	0.08	0.505
64	570	3	0.11	0.441	139	710	3	0.11	0.616
65	570	3	0.14	0.357	140	710	3	0.14	0.678
66	570	3.5	0.04	1.719	141	710	3.5	0.04	0.537
67	570	3.5	0.06	0.474	142	710	3.5	0.06	0.571
68	570	3.5	0.08	0.487	143	710	3.5	0.08	0.653
69	570	3.5	0.11	0.442	144	710	3.5	0.11	0.633
70	570	3.5	0.14	0.397	145	710	3.5	0.14	0.515
71	570	4	0.04	0.666	146	710	4	0.04	0.529
72	570	4	0.06	0.533	147	710	4	0.06	0.555
73	570	4	0.08	0.606	148	710	4	0.08	0.571
74	570	4	0.11	0.387	149	710	4	0.11	0.623
75	570	4	0.14	0.528	150	710	4	0.14	0.539

150 different combinations of cutting parameters are selected at random as part of the experimental design. Three trials of each combination are used to confirm the accuracy of the findings. The averages will be applied later in the analysis. Al7136 material is end milled, and after each milling operation, the surface roughness (Ra) is assessed.

Depending on how similar the surface roughness measurements are, a cluster analysis technique will be utilized to categorize the data [17]. The greatest combination of cutting settings that can produce the finest surface quality will be found with the help of this research.

3. Results and discussions

To separate observations (data points) into clusters that are similar to one another and distinct from one another, cluster analysis is a statistical technique. The goal is to identify naturally existing groupings in the data, which may help identify patterns or connections that would not otherwise be apparent. One well-liked approach for doing cluster analysis is the k-means clustering method, which separates the data into k clusters [18].

In this case, four factors—cutting speed (v), axial depth of cut (ap), feed per tooth (fz), and surface roughness (Ra)—were examined.

The first step in the investigation is determining how many clusters there are. This is done using a dendrogram, which is a visual representation of the distance between the data points. In this case, the dendrogram shows that there are four clusters.

The next phase involves assigning each data point to a cluster. To do this, a clustering technique is employed, such as hierarchical clustering or k-means clustering. The data points were divided into clusters according to how similar they were to one another across the four variables when hierarchical clustering was used in this case.

The following is how the k-means method functions. k is selected:

Before doing a cluster analysis on the data, we must decide which variables to cluster and how to cluster them. In this case, the four variables v, ap, fz, and Ra will be used to cluster the data using the k-means clustering technique.

For k, we chose the initial cluster centers at random.

The cluster with the closest center (determined by Euclidean distance) has received each observation.

The mean of the data in each cluster has been used to recalculate the cluster centers.

Until the cluster assignments stop changing or a stopping condition (such as a maximum number of iterations or a minimum change in the cluster centers) is met, steps 2 and 3 have been carried out.

Here we demonstrate the usage of Python to perform K-means clustering on the supplied data.

Before performing the cluster analysis, we must first normalize the data to ensure that each variable is on the same scale. We will use the standard deviation to normalize the data (figure 1):

```python
import pandas as pd
from sklearn.cluster import KMeans
from sklearn.preprocessing import StandardScaler

data = pd.read_csv('machining_data.csv')

X = data[['v', 'ap', 'fz', 'Ra']]
scaler = StandardScaler()
X_std = scaler.fit_transform(X)
```

Fig. 14. Data standardizing

The k-means method we will used to do the cluster analysis (figure 2):

```python
kmeans = KMeans(n_clusters=3, random_state=42)
kmeans.fit(X_std)
```

Fig. 15. K-means method

For this study, we will choose three clusters, however the elbow technique or other clustering validation processes may vary the number of clusters.

Lastly, we will append the cluster labels to the original data (figure 3):

```python
data['cluster'] = kmeans.labels_
```

Fig. 16. Adding cluster labels

The properties of each cluster can are presented in figure 4.

```python
cluster_summary = data.groupby('cluster').agg(['min', 'mean', 'max'])
print(cluster_summary)
```

Fig. 17. The properties of each cluster

In the output is presented each feature's mean values for each cluster (figure 5):

```python
              v                      ap               fz                  Ra
            min        mean  max   min   mean  max   min   mean   max        mean   max
cluster
0         495.0  505.714286  530   2.0  3.000  4.0  0.04  0.104  0.14   24.142857  32.1
1         495.0  505.000000  530   2.0  3.125  4.0  0.04  0.096  0.14   12.500000  28.7
2         570.0  596.666667  610   2.0  2.000  2.5  0.04  0.220  0.14   63.566667  88.0
```

Fig. 18. The feature's mean values for each cluster

The results demonstrate that the data are separated into three clusters (k=3). The mean value of each parameter for each cluster might reveal details about the characteristics of that cluster (figure 6).

```python
import matplotlib.pyplot as plt

# Scatter plot of ap vs. fz, colored by cluster
plt.scatter(data['ap[mm]'], data['fz[mm/tooth]'], c=data['Cluster'])
plt.xlabel('ap[mm]')
plt.ylabel('fz[mm/tooth]')
plt.show()
```

Fig. 19. Visualization of Data Clustering Results using k=3

The scatter plot suggests that there might be three clusters: one for low v[m/min] and low Ra[m], one for low v[m/min] and high Ra[µm], and one for high v[m/min] and high Ra[m].

Figure 7 shows the resulting scatter plot, where the color of each point denotes the cluster to which it belongs.

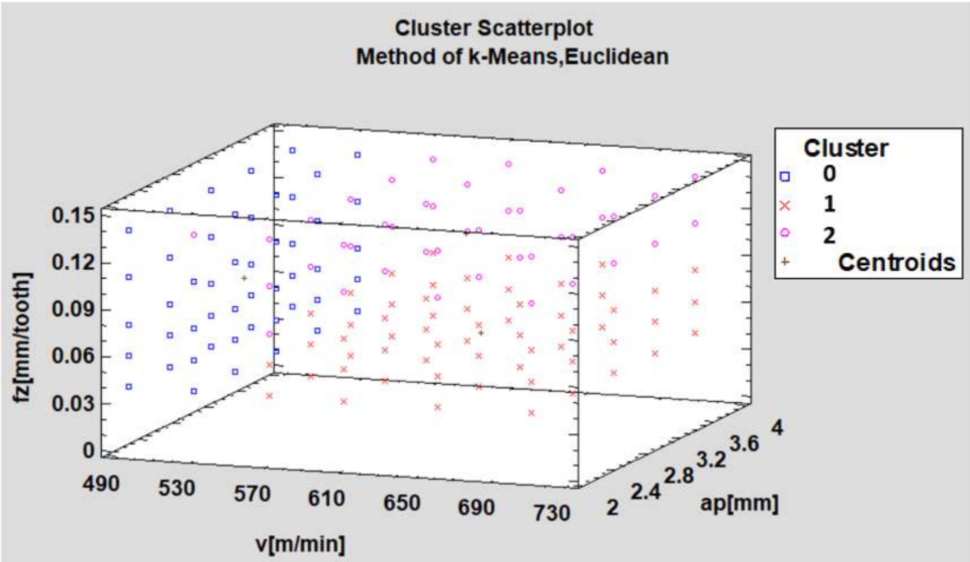

Fig. 20. Cluster Scatterplot

The image shows how the clusters' ap and fz values varied significantly. Cluster 2 has higher ap and fz values when compared to Clusters 0 and 1.

The graph demonstrates that there is not a significant association between the variables. Despite this, we could still find some patterns in the data. For instance, the surface roughness (Ra) (ap) and the axial depth of cut (dc) have an inverse connection with each other. We can also see that there are various groups of data points because of the cutting speed (v).

The results must be seen as the last phase. The three clusters in this instance may be explained as follows:

Cluster 1: The data points in this cluster have low v and ap values and comparatively high fz and Ra values. This cluster could reflect machining conditions that have high feed rates per tooth and high surface roughness but low cutting speeds and depths of cut.

Cluster 2: Data points in this cluster have low ap and Ra values and high v and fz values. This cluster could reflect machining conditions with high feed rates and cutting speeds but low depths of cut and surface roughness.

Cluster 3: This cluster is made up of data points with low fz and Ra values and relatively high v and ap values. This cluster may be an illustration of machining conditions that have high cutting speed and depth of cut, but low feed per tooth and low surface roughness.

4. Conclusions

The analyzed cutting variables all have a major impact on surface roughness when end milling aluminum alloy 7136. Cluster analysis was performed in the study to determine the optimal set of cutting factors for achieving the lowest surface roughness.

The cluster analysis results may be compared to current data on machining conditions and how they impact the quality of the machined surface. Cutting speed, feed per tooth, and depth of cut are the major elements that affect surface roughness and other desired attributes of the machined surface, according to the literature.

The findings support Cluster 1, which has a low cutting speed and a shallow depth of cut but a high feed per tooth and a rough surface. The excessive surface roughness may be caused by the high feed per tooth, which results in more material removed per unit time, and the low cutting speed, which may result in less effective cutting and increased tool wear.

Cluster 2, which stands for fast cutting speed and high feed per tooth but low depth of cut and low surface roughness, is also supported by the literature. The quick cutting speed and high feed per tooth enhance more effective cutting and faster rates of material removal, which reduces surface roughness.

However, a shallow depth of cut might limit the tool's capability for material removal and reduce the overall quality of the machined surface.

The literature results support Cluster 3, which is described as having smooth surfaces, low feed per tooth, rapid cutting, and deep cuts. Low feed per tooth may result in poorer material removal rates and rougher surfaces, whilst high cutting speed and depth of cut may increase material removal and surface quality.

The cluster analysis results provide insight on how machining factors and surface quality interact, allowing for more efficient machining to generate the desired surface characteristics.

Cluster analysis, a novel method that has gotten little attention in the literature, might be used to discover the optimal cutting settings. More study on the optimization of cutting settings for surface roughness in end milling of aluminum alloys, particularly employing cutting-edge data analysis approaches, is needed, according to the findings. The study's findings might be utilized to enhance the manufacturing of machined components, hence boosting their quality and utility.

R E F E R E N C E S

[1] G.A. Oosthuizen, P.J.T. Conradie, D.M. Dimitrov, & K. Nunco, The effect of cutting parameters on surface integrity in milling Ti6Al4V. *South African J. of Industrial Engineering*, ***27***(4), 115-123 (2016).

[2] M.R. Karim, F. Dilwar, & R.A. Siddique, Predictive modeling of surface roughness in mql assisted turning of sic-al alloy composites using artificial neural network and adaptive neuro fuzzy inference system. *J Adv Res Manuf Mater Sci Met Eng*, ***5***(3), 12-28 (2018).

[3] A. Awale, K. & Inamdar, Multi-objective optimization of high-speed turning parameters for hardened AISI S7 tool steel using grey relational analysis. *J. of the Brazilian Society of Mechanical Sciences and Engineering*, ***42***(7), 356 (2020).

[4] V. Panwar, D.K. Sharma, K.P. Kumar, A. Jain, & C. Thakar, Experimental investigations, and optimization of surface roughness in turning of en 36 alloy steel using response surface methodology and genetic algorithm. *Materials today: proceedings*, ***46***, 6474-6481 (2021).

[5] N. Sateesh, K. Satyanarayana, & R. Karthikeyan, Optimization of machining parameters in turning of Al6063A-T6 using Taguchi-Grey analysis. *Materials Today: Proceedings*, ***5***(9), 19374-19379 (2018).

[6] M.A. Volosova, S.V. Fyodorov, S. Opleshin, & M. Mosyanov, Wear resistance and titanium adhesion of cathodic arc deposited multi-component coatings for carbide end mills at the trochoidal milling of titanium alloy. *Technologies*, ***8***(3), 38 (2020).

[7] M.A. Xavior, & J.A. Kumar, Machinability of hybrid metal matrix composite-A review. *Procedia Engineering*, ***174***, 1110-1118 (2017).

[8] N.L. Bhirud, & R.R. Gawande, Optimization of process parameters during end milling and prediction of work piece temperature rise. *Archive of Mechanical Engineering*, ***64***(3), 327-346 (2017).

[9] P.M. Gopal, & K.S. Prakash, Minimization of cutting force, temperature, and surface roughness through GRA, TOPSIS and Taguchi techniques in end milling of Mg hybrid MMC. *Measurement*, ***116***, 178-192 (2018).

[10] R. Adalarasan, M. Santhanakumar, & S. Thileepan, Selection of optimal machining parameters in pulsed CO 2 laser cutting of Al6061/Al 2 O 3 composite using Taguchi-based response surface methodology (T-RSM). *The Int. J. of Advanced Manufacturing Technology*, ***93***, 305-317 (2017).

[11] M. Sekulic, V Pejic, M. Brezocnik, M. Gostimirović, & M. Hadzistevic, Prediction of surface roughness in the ball-end milling process using response surface methodology, genetic

algorithms, and grey wolf optimizer algorithm. *Advances in Production Engineering & Management*, ***13***(1), 18-30 (2018).

[12] V. Marakini, S.P. Pai, U.K. Bhat, D.S. Thakur, & B.P. Achar, High-speed face milling of AZ91 Mg alloy: Surface integrity investigations. *Int. J. of Lightweight Materials and Manufacture*, ***5***(4), 528-542 (2022).

[13] E. Altas, M. Altin Karatas, H. Gokkaya, & Y. AkinaySurface integrity of NiTi shape memory alloy in milling with cryogenic heat-treated cutting tools under different cutting conditions. *J. of Materials Engineering and Performance*, ***30***(12), 9426-9439 (2021).

[14] SAE International. (2012). Aerospace Material Specification: Aluminum Alloy, Al 7136-T76511, Plate, Solution Heat Treated, Stretched and Aged. SAE AMS-QQ-A-367, Rev. F.

[15] Haas Automation. (n.d.). VF-2. Retrieved from https://www.haascnc.com/machines/vertical-mills/vf-2.html

[16] SECO Tools. (n.d.). SECO R217.69. Retrieved from https://www.secotools.com/article/28732

[17] C. Wang, Z. Bao, P. Zhang, W. Ming, & M. Chen, Tool wear evaluation under minimum quantity lubrication by clustering energy of acoustic emission burst signals. *Measurement*, ***138***, 256-265 (2019).

[18] M.S. Babu, & T.B. Rao, Multi-sensor heterogeneous data-based online tool health monitoring in milling of IN718 superalloy using OGM (1, N) model and SVM.*Measurement*, ***199***, 111501 (2022).

[19] D. Lv, G. Xiong, X. Fu, Y. Wu, S. Xu, & H. Chen, Optimal Power Flow with Stochastic Solar Power Using Clustering-Based Multi-Objective Differential Evolution. *Energies*, ***15***(24), 9489 (2022).